Air Filtration

International Edition: DOI: 10.1002/anie.201601782
German Edition: DOI: 10.1002/ange.201601782

Extraordinary NO_2 Removal by the Metal–Organic Framework UiO-66-NH_2

Gregory W. Peterson, John J. Mahle, Jared B. DeCoste, Wesley O. Gordon, and Joseph A. Rossin*

Abstract: *Here we discuss the removal of nitrogen dioxide, an important toxic industrial chemical and pollutant, from air using the MOF UiO-66-NH_2. The amine group is found to substantially aid in the removal, resulting in unprecedented removal capacities upwards of 1.4 g of NO_2/g of MOF. Furthermore, whereas NO_2 typically generates substantial quantities of NO on sorbents, the amount generated by UiO-66-NH_2 is significantly reduced. Of particular significance is the formation of a diazonium ion on the aromatic ring of the MOF, and the potential reduction of NO_2 to molecular nitrogen.*

Nitrogen dioxide, and oxides of nitrogen in general, are among the most common toxic pollutants generated on an annual basis. Typically generated from combustion, nitrogen dioxide is also a common commodity chemical. With the use and generation of NO_x-based chemicals, sorbents are required for their removal, either in flue gas scrubbing operations or protection-based applications. In both, materials must function in both dry and humid conditions. First responders require protection against this material due to its generation from combustion/fires, yet typical respirators containing activated carbon provide limited removal capabilities. A variety of sorbents have been developed and evaluated in the past for the removal of nitrogen dioxide, most notably zeolites[1] and titania. Titania has been evaluated for removing ambient NO_X via photocatalysis.[2]

Metal–organic frameworks (MOFs) are porous sorbents composed of inorganic metal oxide secondary building units (SBUs) connected by polydentate organic linkers. The reticulated network typically provides a high surface area and porosity that has found potential applications in gas storage,[3] separations,[4] sensing,[5] toxic chemical removal,[6] and other areas. In particular, the UiO-66 series of MOFs shows promise for a variety of applications due to its stability against moisture and acidic chemicals,[7] as well as its ability to be processed into useful engineered forms.[8] UiO-66-NH_2 in particular has exhibited extraordinary removal activity for several toxic chemicals of concern. The material has recently been demonstrated to hydrolyze nerve agents at rates competitive with the most active metal oxides.[9] UiO-66-NH_2 was found to remove chlorine via an electrophilic aromatic substitution (EAS) mechanism, resulting in unprecedented chlorine capacities for a solid sorbent.[10] Additional studies have shown UiO-66-NH_2 to be photoactive,[11] further opening the potential for catalytic activity.

Previous studies have investigated UiO-66 for the removal of NO_2. DeCoste synthesized UiO-66 using the missing linker approach[12] and adding oxalic acid at the defect.[13] The resulting material exhibited approximately 8 mol kg^{-1} loading, doubling the capacity as compared to the baseline UiO-66 material. The authors did not discuss the generation of nitric oxide (NO), a common byproduct from the oxidation of surfaces by NO_2. Bandosz and co-workers investigated UiO-66 and the linker-extended version UiO-67 impregnated with urea and melamine.[14,15] In general, NO_2 capacity was found to increase with increasing linker size and the addition of urea. In many cases, however, significant quantities of NO elute, in some cases greater than 30% of the feed, during the test. The maximum loading in these studies was found to be 154 mg NO_2 per g MOF. Cerium was also doped to UiO-66, resulting in modest enhancements to NO_2 removal capacity.[16]

To date, UiO-66-NH_2 has not been investigated for NO_2 removal. In this study, microbreakthrough testing (details are discussed in the Supporting Information (SI) and Figure S1) with NO_2 was conducted on UiO-66 and UiO-66-NH_2 and compared to the activated carbon BPL (Calgon Carbon Corporation), a well-known material often used for toxic gas filtration. Figure 1 shows the breakthrough curves under dry relative humidity conditions. The baseline UiO-66 shows immediate breakthrough, with BPL carbon eluting soon after. Both materials do exhibit capacity, however, as they take quite long to reach saturation on a weighted time scale. UiO-66-NH_2 takes much longer to elute, and the breakthrough curves exhibit significantly more capacity than the other materials evaluated, as summarized in Table 1. Approximately 7 wt% of NO is produced by the interaction of NO_2 with UiO-66-NH_2, significantly less than the 28% generated by BPL carbon. The resulting capacity for UiO-66-NH_2 is 0.9 g NO_2 g^{-1} to saturation.

Each material was also challenged with NO_2 at a relative humidity of 80%. Microbreakthrough curves are shown in Figure S2, and results are summarized in Table 1. In this case, we see NO_2 elute to significant quantities almost immediately; this behaviour may be due to competition with moisture within the pore structure, thus reducing diffusion rates to the active sites. Although BPL does show initial capacity for NO_2,

[*] G. W. Peterson, J. J. Mahle, J. B. DeCoste, W. O. Gordon
Edgewood Chemical Biological Center
5183 Blackhawk Rd., Aberdeen Proving Ground, MD 21010 (USA)
E-mail: gregory.w.peterson.civ@mail.mil
J. A. Rossin
Guild Associates, Inc.
5750 Shier Rings Road, Dublin, OH 43016 (USA)

Supporting information for this article can be found under: http://dx.doi.org/10.1002/anie.201601782.

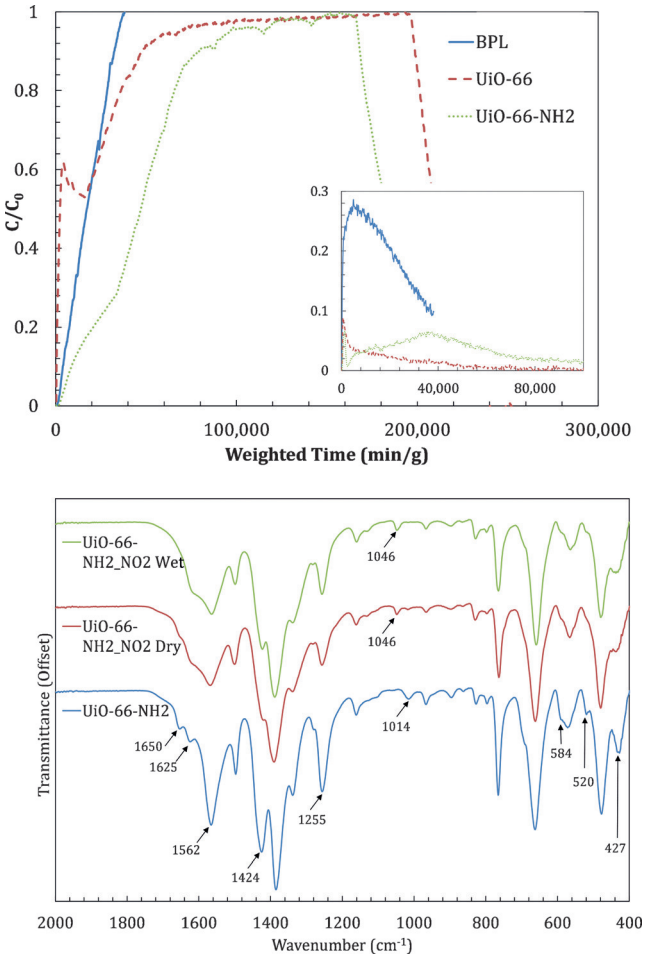

Figure 1. NO_2 microbreakthrough curves (top) under dry RH, with NO elution inset. Results are presented as weighted time, which is time divided by sorbent mass, to account for differences in material density.

Table 1: Nitrogen dioxide capacities for various materials.

Condition	Parameter	Values BPL	UiO-66	UiO-66-NH_2
Dry[a]	mol kg^{-1}	8.8	8.8	20.3
	g NO_2 g^{-1} MOF	0.40	0.40	0.93
	% NO generated	28	9.0	6.8
Humid[b]	mol kg^{-1}	15.6	13.2	31.2
	g NO_2 g^{-1} MOF	0.72	0.61	1.4
	% NO generated	23	9.5	4.5

[a] Sample activated at 150°C, tested at 0% RH. [b] Sample equilibrated at 80% RH, tested at 80% RH.

it quickly reaches saturation whereas both MOFs take significantly longer to reach the feed concentration. The amount of NO generated under humid conditions is lower than in dry conditions for UiO-66-NH_2, perhaps due to preferential formation of nitrous acid. The resulting loading is over 1.4 g NO_2 per g at saturation. The substantially increased loading for both BPL and UiO-66-NH_2 can be attributed to the significantly higher water content in each at 80% RH, which aids in the reaction of NO_2. The relatively lower increase for UiO-66 follows the lower water content at 80% RH (Figure S3). For comparison, testing shows almost no capacity for H- and Na-ZSM-5 under humid conditions. HKUST-1 shows 0.3 and 1.2 g NO_2/g MOF under dry and humid conditions, respectively, but with significant NO generation.

Attenuated total reflectance Fourier Transform infrared (ATR FTIR) data in Figure 1 begin to show how the baseline UiO-66-NH_2 structure is affected by NO_2. Peaks in the region of 1650–1560 cm^{-1} from aryl amines are reduced/broadened after exposure, indicating that the NH_2 group is active in the removal process. This is consistent with previous studies where urea interacted with NO_2.[14] Additional peaks in the range of 600–425 cm^{-1} due to metal oxide bonds in the secondary building unit (SBU) also decrease, indicating that there is some reaction of NO_2 at the SBU. Yet there are no noticeable differences in the powder X-ray diffraction data (Figure S4), indicating any reaction is localized and not abundant throughout the material, or there is no framework bond breakage in the material. Nitrogen isotherm data (Figure S5) further support this hypothesis; although there is a decrease in nitrogen adsorption after NO_2 exposure, a significant amount of surface area and porosity still exist (Table S1), indicating that the structure remains intact.

^{1}H NMR spectra of acid digested UiO-66-NH_2 exposed to NO_2 show that the 2-aminoterephthalic acid linker remains largely unperturbed (Figure S6). However, there is the appearance of new peaks in the region from 7.8 to 8.2 ppm, potentially representing a partially nitrated ring. When examining the diffuse reflectance infrared Fourier transform spectroscopy (DRIFTS) data (Figure S7) for UiO-66-NH_2 exposed to NO_2, two major features are apparent. The first is a strong loss of the -OH group at 3675 cm^{-1} (Figure S8), these groups are likely bound to the SBU. The most noticeable new band, however, occurs at 2280 cm^{-1}, shown in Figure 2, which is representative of a diazonium salt.[17] This was confirmed by exposing UiO-66-NH_2 to $NaNO_2$ in 6 M HCl, showing the same characteristic IR band. Further evidence is shown by the decrease in asymmetric and symmetric N–H stretches at 3514 and 3397 cm^{-1}, respectively.

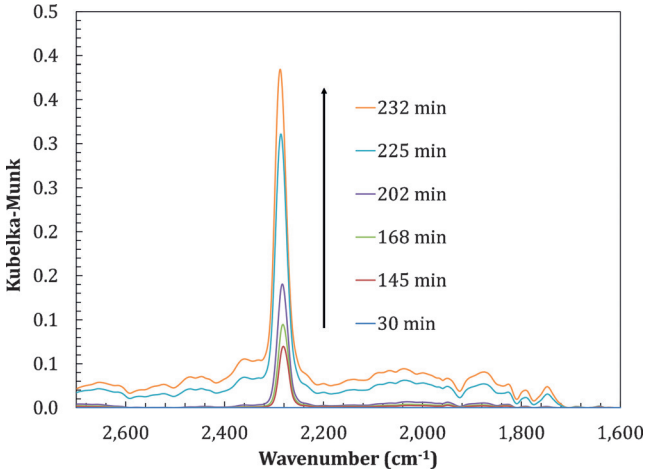

Figure 2. DRIFTS Spectra for UiO-66-NH_2 exposed to NO_2 as a function of time.

Data in the fingerprint region confirm earlier ATR-FTIR analysis, as additional peaks indicate the presence of physically adsorbed NO_2.

X-ray photoelectron spectroscopy (XPS) data were used to further elucidate the mechanism. Figure 3 shows the nitrogen 1s region for UiO-66-NH_2 before and after NO_2 exposure. As compared to the baseline sample, peaks at approximately 407.2 eV are seen after exposure to NO_2,

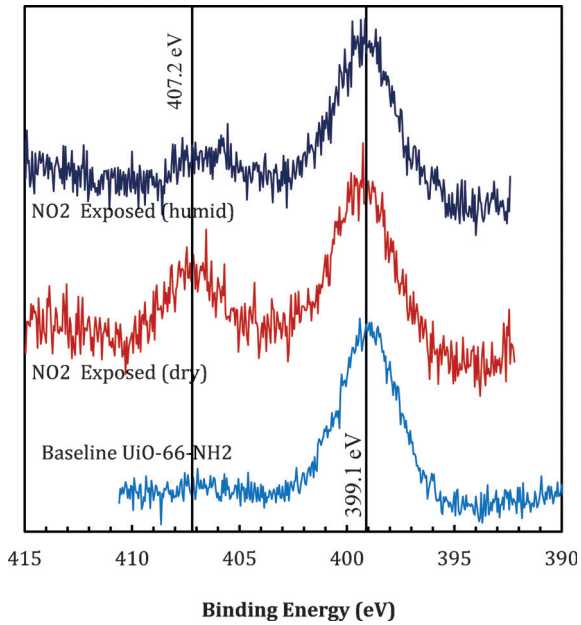

Figure 3. Nitrogen 1s XPS data for UiO-66-NH_2 for as-received and exposed samples.

indicative of nitrate species. The peak is more pronounced for the sample exposed under dry conditions as compared to humid conditions, and the resulting atomic ratios shown in Table S2 confirm the result. Compared to the baseline UiO-66, the amine version retains twice as much nitrogen as nitrate, commensurate with the increased loading demonstrated from breakthrough testing. Interestingly, the nitrogen content associated with the amine goes down after exposure, as shown by the atomic ratios in Table S2, indicating that NO_2 may react at that site. The reduction in carbon 1s peaks after exposure (Figure S10) also indicates potential interaction at the carboxylate, although CO and CO_2 measurements using FTIR showed little evidence of oxidation.[18]

Coupling the various characterization techniques, we propose that NO_2 is removed by UiO-66-NH_2 via several mechanisms, as summarized in Figure 4. NO_2 first adsorbs within the pores of the MOF. This is supported by temperature-dependant data shown in Figure S13 and DRIFTS analysis. Loading increases with decreasing temperature, indicating that physical adsorption has a major impact on removal. Once adsorbed, the chemical reacts with the organic linker in multiple locations. Previous reports show that NO_2 is added stoichiometrically to benzene rings at temperatures slightly above ambient, forming nitric acid.[19] A decrease of C–H on the aromatic ring as shown by ATR supports this

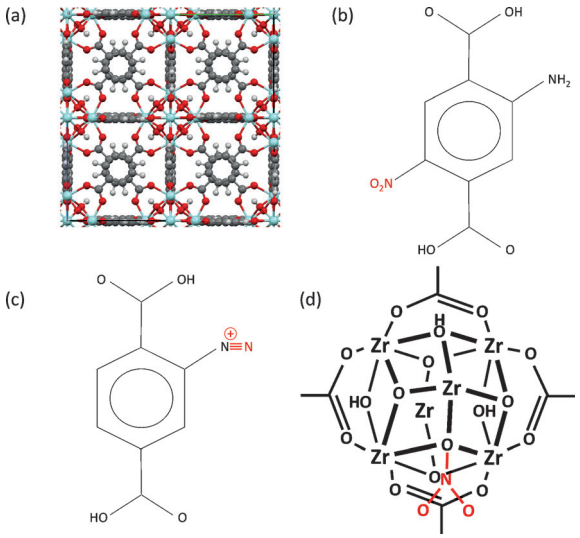

Figure 4. a) The structure of UiO-66 analogs, b) nitration of the benzene ring, c) diazonium ion formation, and d) nitration of the bridging hydroxyl at the SBU.

reaction. A diazonium ion is also formed at the amine group, which was shown by DRIFTS. This behavior is supported by atomic ratios calculated from XPS data, where it is shown that nitrogen associated with the amine group is actually reduced compared to the baseline material. The amine group may also be responsible for forming complexes with NO_2 and any NO generated by other reactions, such as interaction with water.[20]

Finally, NO_2, HNO_2 generated from moisture, and/or HNO_3 generated from reaction with the linker further reacts at the SBU, as seen by XPS. Because the structure remains intact, the likely reaction occurring is nitrate formation at the bridging oxygen of the SBU. Even considering the multitude of products formed, the overall mass balance of nitrogen still does not quite close; this indicates that molecular nitrogen may also be formed in this reaction, which has been shown to occur by dissociation of diazonium ions.[21]

In conclusion, we have shown that UiO-66-NH_2 removes the toxic gas nitrogen dioxide at extraordinary levels while minimizing nitric oxide byproduct formation compared to activated carbons. In fact, no other material is known to provide such high nitrogen dioxide removal capacities. The complicated mechanism directly results from the multitude of active sites present on the MOF, including the exciting reaction of a diazonium ion from a gas phase reaction. The astonishing loadings achieved by UiO-66-NH_2 provide further evidence of the potential usefulness of this MOF in protection applications.

Acknowledgements

G.W.P. thanks the Joint Science and Technology Office for Chemical Biological Defense for funding under project number BA07PRO104, as well as David K. Britt (LBNL) for synthesizing UiO-66-NH_2.

Keywords: diazonium ion · filtration · metal–organic framework · nitrogen dioxide · UiO-66-NH_2

How to cite: *Angew. Chem. Int. Ed.* **2016**, *55*, 6235 – 6238
Angew. Chem. **2016**, *128*, 6343 – 6346

[1] T. C. Brüggemann, M.-D. Przybylski, S. P. Balaji, F. J. Keil, *J. Phys. Chem. C* **2010**, *114*, 6567 – 6587; K. Smith, S. Almeer, S. J. Black, *Chem. Commun.* **2000**, 1571 – 1572; J. O. Petunchi, W. K. Hall, *Appl. Catal. B* **1993**, *2*, L17 – L26.

[2] M. E. Monge, B. D′Anna, C. George, *Phys. Chem. Chem. Phys.* **2010**, *12*, 8991 – 8998.

[3] R. B. Getman, Y.-S. Bae, C. E. Wilmer, R. Q. Snurr, *Chem. Rev.* **2012**, *112*, 703 – 723; S. S. Han, J. L. Mendoza-Cortes, W. A. Goddard III, *Chem. Soc. Rev.* **2009**, *38*, 1460 – 1476; J. B. DeCoste, M. H. Weston, P. E. Fuller, T. M. Tovar, G. W. Peterson, M. D. LeVan, O. K. Farha, *Angew. Chem. Int. Ed.* **2014**, *53*, 14092 – 14095; *Angew. Chem.* **2014**, *126*, 14316 – 14319.

[4] K. Sumida, D. L. Rogow, J. A. Mason, T. M. McDonald, E. D. Bloch, Z. R. Herm, T.-H. Bae, J. R. Long, *Chem. Rev.* **2012**, *112*, 724 – 781; J.-R. Li, J. Sculley, H.-C. Zhou, *Chem. Rev.* **2012**, *112*, 869 – 932.

[5] J. A. Greathouse, N. W. Ockwig, L. J. Criscenti, T. R. Guilinger, P. Pohl, M. D. Allendorf, *Phys. Chem. Chem. Phys.* **2010**, *12*, 12621 – 12629; L. E. Kreno, K. Leong, O. K. Farha, M. Allendorf, R. P. Van Duyne, J. T. Hupp, *Chem. Rev.* **2012**, *112*, 1105 – 1125.

[6] J. B. DeCoste, G. W. Peterson, *Chem. Rev.* **2014**, *114*, 5695 – 5727; E. Barea, C. Montoro, J. A. R. Navarro, *Chem. Soc. Rev.* **2014**, *43*, 5419 – 5430.

[7] J. H. Cavka, S. Jakobsen, U. Olsbye, N. Guillou, C. Lamberti, S. Bordiga, K. P. Lillerud, *J. Am. Chem. Soc.* **2008**, *130*, 13850 – 13851; J. B. DeCoste, G. W. Peterson, H. Jasuja, T. G. Glover, Y.-g. Huang, K. S. Walton, *J. Mater. Chem. A* **2013**, *1*, 5642 – 5650.

[8] G. W. Peterson, J. B. DeCoste, T. G. Glover, Y. Huang, H. Jasuja, K. S. Walton, *Microporous Mesoporous Mater.* **2013**, *179*, 48 – 53; G. W. Peterson, J. B. DeCoste, F. Fatollahi-Fard, D. K. Britt, *Ind. Eng. Chem. Res.* **2014**, *53*, 701 – 707.

[9] J. E. Mondloch, M. J. Katz, W. C. Isley III, P. Ghosh, P. Liao, W. Bury, G. W. Wagner, M. G. Hall, J. B. DeCoste, G. W. Peterson, R. Q. Snurr, C. J. Cramer, J. T. Hupp, O. K. Farha, *Nat. Mater.* **2015**, *14*, 512 – 516; T. J. Bandosz, M. Laskoski, J. Mahle, G. Mogilevsky, G. W. Peterson, J. A. Rossin, G. W. Wagner, *J. Phys. Chem. C* **2012**, *116*, 11606 – 11614.

[10] J. B. DeCoste, M. A. Browe, G. W. Wagner, J. A. Rossin, G. W. Peterson, *Chem. Commun.* **2015**, *51*, 12474 – 12477.

[11] L. Shen, S. Liang, W. Wu, R. Liang, L. Wu, *Dalton Trans.* **2013**, *42*, 13649 – 13657; J. Long, S. Wang, Z. Ding, S. Wang, Y. Zhou, L. Huang, X. Wang, *Chem. Commun.* **2012**, *48*, 11656 – 11658.

[12] M. Vandichel, J. Hajek, F. Vermoortele, M. Waroquier, D. E. De Vos, V. Van Speybroeck, *CrystEngComm* **2015**, *17*, 395 – 406; H. Wu, Y. S. Chua, V. Krungleviciute, M. Tyagi, P. Chen, T. Yildirim, W. Zhou, *J. Am. Chem. Soc.* **2013**, *135*, 10525 – 10532.

[13] J. B. DeCoste, T. J. Demasky, M. J. Katz, O. K. Farha, J. T. Hupp, *New J. Chem.* **2015**, *39*, 2396 – 2399.

[14] A. M. Ebrahim, T. J. Bandosz, *Microporous Mesoporous Mater.* **2014**, *188*, 149 – 162.

[15] A. M. Ebrahim, B. Levasseur, T. J. Bandosz, *Langmuir* **2013**, *29*, 168 – 174.

[16] A. M. Ebrahim, T. J. Bandosz, *ACS Appl. Mater. Interfaces* **2013**, *5*, 10565 – 10573.

[17] K. Tabei, C. Ito, *Bull. Chem. Soc. Jpn.* **1968**, *41*, 514.

[18] E. Johansson, L. Nyborg, *Surf. Interface Anal.* **2003**, *35*, 375 – 381.

[19] P. Gray, A. D. Yoffe, *Chem. Rev.* **1955**, *55*, 1069 – 1154.

[20] Y.-L. Zhao, S. L. Garrison, C. Gonzalez, W. D. Thweatt, M. Marquez, *J. Phys. Chem. A* **2007**, *111*, 2200 – 2205.

[21] S. Dahmen, S. Brase, *Angew. Chem. Int. Ed.* **2000**, *39*, 3681 – 3683; *Angew. Chem.* **2000**, *112*, 3827 – 3830.

Received: February 19, 2016
Published online: April 13, 2016

